

## Low-Temperature N–O Bond Cleavage in Nitrosyl Ligands Induced by the Unsaturated Dimolybdenum Anion $[\text{Mo}_2(\eta^5\text{-C}_5\text{H}_5)_2(\mu\text{-PPh}_2)(\mu\text{-CO})_2]^-$

M. Esther García,<sup>†</sup> Daniel García-Vivó,<sup>†</sup> Sonia Melón,<sup>†</sup> Miguel A. Ruiz,<sup>\*,†</sup> Claudia Graiff,<sup>‡</sup> and Antonio Tiripicchio<sup>‡</sup>

<sup>†</sup>*Departamento de Química Orgánica e Inorgánica/IUQOEM, Universidad de Oviedo, E-33071 Oviedo, Spain, and* <sup>‡</sup>*Dipartimento di Chimica Generale ed Inorganica, Chimica Analitica, Chimica Fisica, Università di Parma, Viale G. P. Usberti 17/A, I-43100 Parma, Italy*

Received June 10, 2009

The unsaturated anion  $[\text{Mo}_2\text{Cp}_2(\mu\text{-PPh}_2)(\mu\text{-CO})_2]^-$  (**1**) ( $\text{Na}^+$  salt) reacts with the nitrosyl complexes  $[\text{MCp}'(\text{CO})_2(\text{NO})]\text{BF}_4$  ( $\text{M} = \text{Mn, Re}$ ;  $\text{Cp}' = \eta^5\text{-C}_5\text{H}_4\text{Me}$ ) rapidly at about 193 K. Upon warming of the resulting mixtures up to 243 K orange solutions are obtained, shown to contain the corresponding oxo- and nitride-bridged tetracarbonyl complexes  $[\text{Mo}_2\text{MCp}_2\text{Cp}'(\mu\text{-N})(\mu\text{-O})(\mu\text{-PPh}_2)(\text{CO})_4]$  as the major product, which could be isolated only for  $\text{M} = \text{Re}$ . Above 253 K, however, these compounds experience spontaneous decarbonylation to yield the unsaturated tricarbonyl derivatives  $[\text{Mo}_2\text{MCp}_2\text{Cp}'(\mu\text{-N})(\mu\text{-O})(\mu\text{-PPh}_2)(\text{CO})_3]$  ( $\text{Mo}\text{--}\text{Mo} = 2.840 \text{ \AA}$  for the Mn compound, according to density functional theory (DFT) calculations). These complexes in turn react rapidly with air to give the corresponding dioxodicarbonyl derivatives  $[\text{Mo}_2\text{MCp}_2\text{Cp}'(\mu\text{-N})(\mu\text{-O})(\mu\text{-PPh}_2)(\text{O})(\text{CO})_2]$  almost quantitatively. The structure of the latter product ( $\text{M} = \text{Re}$ ) was determined by X-ray diffraction methods ( $\text{Mo}\text{--}\text{Mo} = 2.763(1) \text{ \AA}$ ). In contrast with the N–O bond cleavage easily taking place in the above reactions, the direct nitrosylation of **1** with *N*-methyl-*N*-nitroso-*p*-toluenesulfonamide induces no bond cleavage process in the nitrosyl ligand, but just gives the electron-precise tricarbonyl derivative  $[\text{Mo}_2\text{Cp}_2(\mu\text{-PPh}_2)(\text{CO})_3(\text{NO})]$  or, in the presence of  $\text{CN}^t\text{Bu}$ , a mixture of the new isocyanide complexes  $[\text{Mo}_2\text{Cp}_2(\mu\text{-PPh}_2)(\text{CN}^t\text{Bu})(\text{CO})_2(\text{NO})]$  and  $[\text{Mo}_2\text{Cp}_2(\mu\text{-PPh}_2)(\mu\text{-}\eta^1\text{:}\eta^2\text{-CN}^t\text{Bu})(\text{CO})(\text{NO})]$ . Separate experiments indicated that these isocyanide complexes cannot be converted one into each other, nor can they be obtained through thermal substitution reactions on the above tricarbonyl product.

### Introduction

Nitrogen monoxide is a remarkable molecule able to strongly bind to transition metal atoms both in high and low oxidation states, thus giving rise to a wide variety of coordination and organometallic complexes exhibiting a rich

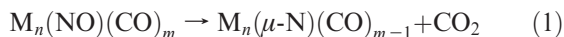
chemistry.<sup>1,2</sup> Further interest in this molecule stems from its biological activity,<sup>1,3</sup> and also because nitrogen monoxide is one of the important air pollutants requiring catalytic abatement.<sup>1,4,5</sup> The activation and cleavage of the strong N–O bond of nitrogen monoxide when bound to a metal atom then is a process of particular relevance to understanding the biological role of this molecule and also to developing better catalysts for its abatement in diverse gas effluents. In this context we have carried out a prospective study on this important reaction using different binuclear carbonyl complexes as potential activators of the N–O bond of the nitrosyl ligand.

The ability of organometallic compounds to cleave the N–O bond of the nitrosyl ligand is known, but the electronic and steric factors governing this fundamental reaction remain unclear in most cases. For example, it is not unusual that the treatment of carbonyl clusters with several sources of the NO ligand would lead to the corresponding nitride

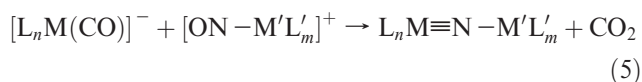
\*To whom correspondence should be addressed. E-mail: mara@uniovi.es.  
(1) Ritcher-Addo, G. B.; Legzdins, P. *Metal Nitrosyls*; Oxford University Press: Oxford, U.K., 1992.  
(2) (a) Hayton, T. W.; Legzdins, P.; Sharp, W. B. *Chem. Rev.* **2002**, *102*, 935. (b) Ford, P. C.; Lorkovic, I. M. *Chem. Rev.* **2002**, *102*, 993. (c) Mingos, D. M. P.; Sherman, D. J. *Adv. Inorg. Chem.* **1989**, *34*, 293. (d) Gladfelter, W. L. *Adv. Organomet. Chem.* **1985**, *24*, 41.  
(3) (a) Franke, A.; Roncaroli, F.; Rudi, v. E. *Eur. J. Inorg. Chem.* **2007**, 773. (b) Ghosh, A. *Acc. Chem. Res.* **2005**, *38*, 943. (c) Ford, P. C.; Laverman, L.; Lorkovic, I. M. *Adv. Inorg. Chem.* **2003**, *54*, 203. (d) Wang, P. G.; Xian, M.; Tang, X.; Wu, X.; Wen, Z.; Cai, T.; Janczuk, A. *J. Chem. Rev.* **2002**, *102*, 1091. (e) Butler, A. R.; Megson, I. L. *Chem. Rev.* **2002**, *102*, 1155. (f) Williams, R. J. P. *Chem. Soc. Rev.* **1996**, *77*. (g) Clarke, M. J.; Gaul, J. B. *Struct. Bonding (Berlin)* **1993**, *81*, 147.  
(4) (a) *Reduction of Nitrogen Oxide Emissions*; Ozkan, U. S., Agarwal, S. K., Marcelin, G., Eds.; American Chemical Society: Washington, DC, 1995. (b) *Environmental Catalysis*; Armor, J. M., Ed.; American Chemical Society: Washington, DC, 1994. (c) *Catalytic Control of Air Pollution*; Silver, R. G., Sawyer, J. E., Summers, J. C., Eds.; American Chemical Society: Washington, DC, 1992. (d) *Energy and the Environment*; Dunderdale, J., Ed.; Royal Society of Chemistry: Cambridge, U.K., 1990. (e) *Pollution: Causes, Effects and Control*; Harrison, R. M., Ed.; Royal Society of Chemistry: Cambridge, U.K., 1990.

(5) (a) Basu, S. *Chem. Eng. Commun.* **2007**, *194*, 1374. (b) Tayyeb, J. M.; Naseem, I.; Gibbs, B. M. *J. Environ. Manage.* **2007**, *83*, 251. (c) Wallington, T. J.; Kaiser, E. W.; Farrell, J. T. *Chem. Soc. Rev.* **2006**, *35*, 335. (d) McMillan, S. A.; Broadbelt, L. J.; Snurr, R. Q. *Environ. Catal.* **2005**, 287. (e) Curtin, T. *Environ. Catal.* **2005**, 197.

(rather than nitrosyl) derivatives.<sup>2c,d,6</sup> However, even when intermediate nitrosyl complexes are expected to be involved in these reactions, the actual transformation of a well-defined nitrosyl complex into the corresponding nitride derivative has been rarely observed (eq 1).<sup>7</sup> A few other reactions involving the cleavage of the N–O bond by metals in well-defined organometallic nitrosyl complexes have been reported, all of these involving electron-deficient centers, either binuclear (eq 2),<sup>8</sup> or mononuclear ones (eq 3).<sup>9</sup> Yet, another reported cleavage process is the abstraction of the oxygen atom of a terminal nitrosyl ligand by a strongly oxophilic complex (eq 4),<sup>10</sup> this reaction being specially favored for M and M' having d<sup>3</sup> and d<sup>2</sup> configurations respectively, according to recent density functional theory (DFT) calculations.<sup>11</sup>



Recently we reported that the reactions of several anionic complexes of the group 6 metals  $[\text{MCp}(\text{CO})_2\text{L}]^-$  ( $\text{Na}^+$  or  $\text{K}^+$  salts; M = Mo, W; Cp =  $\eta^5\text{-C}_5\text{H}_5$ ; L = CO, P(OMe)<sub>3</sub>, PPh<sub>3</sub>) with the electron-precise nitrosyl cations  $[\text{M}'\text{Cp}'(\text{CO})_2(\text{NO})]^+$  ( $\text{BF}_4^-$  salts; M' = Mn, Re; Cp' =  $\eta^5\text{-C}_5\text{H}_4\text{Me}$ ) take place readily at low temperatures and lead to the heterometallic nitride-bridged derivatives  $[\text{MM}'\text{CpCp}'(\mu\text{-N})(\text{CO})_3\text{L}]$ .<sup>12</sup> A DFT study of the likely pathways involved in these reactions revealed that the N–O bond cleavage process yielding the nitride derivative follows from the orbitally controlled nucleophilic attack of the anion to the nitrogen atom of the nitrosyl ligand in the cation, eventually releasing CO<sub>2</sub> (eq 5). We should note that this reaction pathway appears to have been not recognized previously in the chemistry of polynuclear complexes having carbonyl or nitrosyl ligands.



Our calculations on the above reactions suggested that the elimination of CO<sub>2</sub> (a major thermodynamic driving force for

this reaction) was kinetically favored because of the close proximity between CO and NO ligands in the intermediate states, this being facilitated by the presence of three CO ligands (or the equivalent) in the anionic group 6 metal complex.<sup>12</sup> With this precedent in mind we then considered the possibility of using group 6 metal carbonyl anions having fewer ligands at the metal so as to achieve an N–O bond cleavage process without release of CO<sub>2</sub>. In this paper we report our results on the reactions of the unsaturated anion  $[\text{Mo}_2\text{Cp}_2(\mu\text{-PPh}_2)(\mu\text{-CO})_2]^-$  (**1**) ( $\text{Na}^+$  salt, Chart 1)<sup>13</sup> with the mentioned nitrosyl cations  $[\text{M}'\text{Cp}'(\text{CO})_2(\text{NO})]^+$ , which indeed lead to the full cleavage of the nitrosyl N–O bond to give the corresponding oxonitride heterometallic derivatives. The bonding in the latter complexes has been examined using DFT methods. We next examined the direct nitrosylation reactions of **1** to check whether the electronic and coordinative unsaturation of this anion would be enough to induce the cleavage of the nitrosyl ligand, but these reactions gave only different nitrosyl derivatives, as it will be discussed below.

## Results and Discussion

**Reactions of Compound 1 with Nitrosyl Complexes.** The unsaturated anion **1** reacts in tetrahydrofuran (THF) solution with several nitrosyl complexes susceptible to act as sources of cationic nitrosyl metal fragments, such as the compounds  $[\text{CoCpX}(\text{NO})]$  (X = Cl, I) and  $[\text{MCpCl}(\text{NO})_2]$  (M = Mo, W) or related species, but complex mixtures of products were obtained in all cases, these including the previously reported compounds  $[\text{Mo}_2\text{Cp}_2(\mu\text{-Cl})(\mu\text{-PPh}_2)(\text{CO})_2]^{13}$  and  $[\text{Mo}_2\text{Cp}_2(\mu\text{-PPh}_2)(\text{CO})_3(\text{NO})]$ ,<sup>14</sup> then suggesting the operation of several electron-transfer processes involving halogen and nitrosyl transfer to the unsaturated dimolybdenum center. In contrast, the reaction of **1** with the rhenium salt  $[\text{ReCp}'(\text{CO})_2(\text{NO})]\text{BF}_4$  was found to be quite selective. The latter takes place rapidly at about 193 K, since a black-green solution is instantaneously formed upon mixing of the reagents at that temperature. Upon warming the mixture up to 243 K over 30 min, an orange solution is formed, shown to contain the nitride tetracarbonyl complex  $[\text{Mo}_2\text{ReCp}_2\text{Cp}'(\mu\text{-N})(\mu\text{-O})(\mu\text{-PPh}_2)(\text{CO})_4]$  (**2a**) as the major product (Scheme 1).

Compound **2a** can be isolated as a solid from the reaction mixture in the usual way, as long as the temperature is kept below 253 K. Above this temperature, however, an spontaneous decarbonylation takes place to yield the unsaturated tricarbonyl derivative  $[\text{Mo}_2\text{ReCp}_2\text{Cp}'(\mu\text{-N})(\mu\text{-O})(\mu\text{-PPh}_2)(\text{CO})_3]$  (**3a**) almost quantitatively. According to the EAN formalism we might formulate a molybdenum–molybdenum double or a single bond for this molecule, depending on the electron-donor ability of the bridging oxygen atom, a question to be addressed later on in the light of DFT calculations. In any case, this complex turns out to be very air-sensitive, and it progressively evolves upon manipulation (rapidly in the presence of air) to give the dioxodicarbonyl derivative  $[\text{Mo}_2\text{ReCp}_2\text{Cp}'(\mu\text{-N})(\mu\text{-O})(\mu\text{-PPh}_2)(\text{O})(\text{CO})_2]$  (**4a**) in quite good yield, presumably with evolution of CO<sub>2</sub>, as it is usually

(6) For a recent work on this matter see: Babij, C.; Farrar, D. H.; Pöe, A. J.; Tunik, S. P. *Dalton Trans.* **2008**, 5922.

(7) (a) Fjare, D. E.; Gladfelter, W. L. *J. Am. Chem. Soc.* **1984**, *106*, 4799. (b) Feasey, N. D.; Knox, S. A. R.; Orpen, A. G. *J. Chem. Soc., Chem. Commun.* **1982**, 75.

(8) Legzdins, P.; Young, M. A. *Comments Inorg. Chem.* **1995**, *17*, 239.

(9) (a) Blackmore, I. J.; Jin, X.; Legzdins, P. *Organometallics* **2005**, *24*, 4088. (b) Sharp, W. B.; Daff, P. J.; McNeil, W. S.; Legzdins, P. *J. Am. Chem. Soc.* **2001**, *123*, 6272.

(10) (a) Veige, A. S.; Slaughter, LeG. M.; Lobkovsky, E. B.; Wolczansky, P. T.; Matsunaga, N.; Decker, S. A.; Cundari, T. R. *Inorg. Chem.* **2003**, *42*, 6204. (b) Odom, A. L.; Cummins, C. C.; Protasiewicz, J. D. *J. Am. Chem. Soc.* **1995**, *117*, 6613.

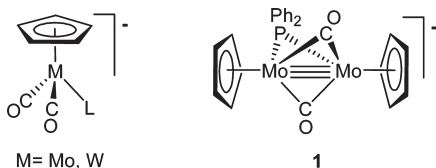
(11) Cavigliasso, G.; Christian, G.; Stranger, R.; Yates, B. F. *Dalton Trans.* **2009**, 956.

(12) García, M. E.; Melón, S.; Ruiz, M. A.; López, R.; Sordo, T.; Marchiò, L.; Tiripicchio, A. *Inorg. Chem.* **2008**, *47*, 10644.

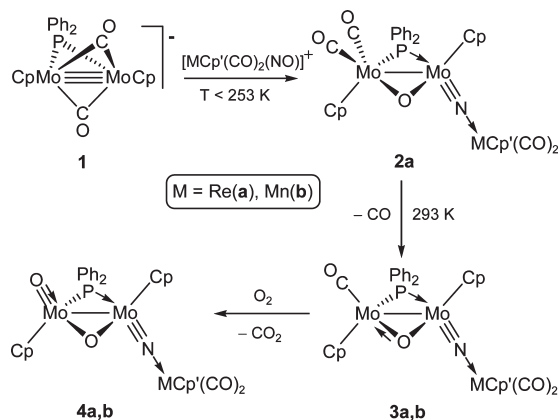
(13) García, M. E.; Melón, S.; Ramos, A.; Riera, V.; Ruiz, M. A.; Belletti, D.; Graiff, C.; Tiripicchio, A. *Organometallics* **2003**, *22*, 1983.

(14) García, M. E.; Riera, V.; Rueda, M. T.; Ruiz, M. A.; Lanfranchi, M.; Tiripicchio, A. *J. Am. Chem. Soc.* **1999**, *121*, 4060.

Chart 1



Scheme 1



the case in the oxidation reactions of many metal carbonyls. The assignment of the intermetallic bond order in this dioxonitride complex again is not a straightforward matter, and this will be addressed in the light of the structural data to be discussed below.

The reaction of **1** with the manganese salt  $[\text{MnCp}'(\text{CO})_2(\text{NO})]\text{BF}_4$  was much less selective than the one with the rhenium cation just discussed, and several side-products were detected, these including known binuclear products such as the nitrosyl  $[\text{Mo}_2\text{Cp}_2(\mu\text{-PPh}_2)(\text{CO})_3(\text{NO})]$ ,<sup>14</sup> the hydride  $[\text{Mo}_2\text{Cp}_2(\mu\text{-H})(\mu\text{-PPh}_2)(\text{CO})_4]$ ,<sup>15</sup> and the dimer  $[\text{Mn}_2\text{Cp}'_2(\text{CO})_2(\text{NO})_2]$ .<sup>16</sup> Thus, it is obvious that electron-transfer processes become more prevalent in the reaction with the manganese cation. Besides, we could detect spectroscopically the formation of an intermediate species comparable to the tetracarbonyl **2a**, but apparently this complex is even more unstable than its rhenium analogue, and it rapidly dissociates carbon monoxide to give the tricarbonyl derivative  $[\text{Mo}_2\text{MnCp}_2\text{Cp}'(\mu\text{-N})(\mu\text{-O})(\mu\text{-PPh}_2)(\text{CO})_3]$  (**3b**), which is the only new product that we could isolate from the reaction mixture, even if in a modest yield (ca. 25%). Compound **3b** seems to have the same structure as the rhenium tricarbonyl **3a**, a matter to be discussed later on, and it is also very air-sensitive, since it reacts rapidly with air to give the corresponding dioxodicarbonyl derivative  $[\text{Mo}_2\text{MnCp}_2\text{Cp}'(\mu\text{-N})(\mu\text{-O})(\mu\text{-PPh}_2)(\text{O})(\text{CO})_2]$  (**4b**) in good yield. The structure and bonding of **3b** has been theoretically analyzed using DFT methods, as it will be discussed later on.

**Solid-State Structure of the Nitride Complex 4a.** The molecular structure of this complex in the crystal is shown in Figure 1, while the most relevant bond lengths and angles are collected in Table 1. The molecule can be

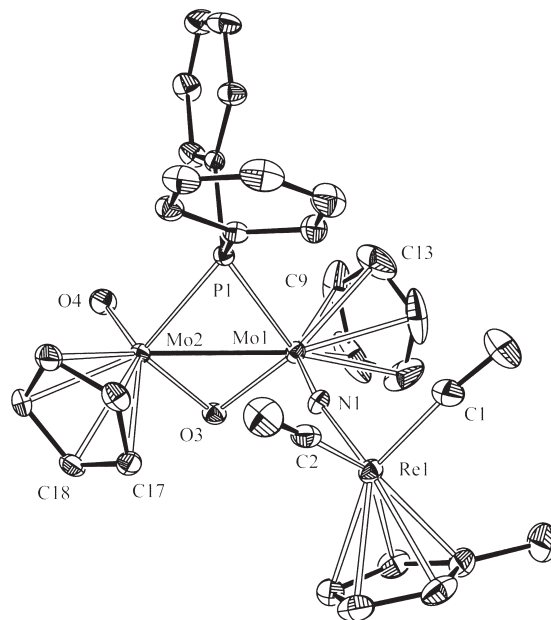


**Figure 1.** ORTEP drawing (30% probability) of the molecular structure of compound **4a**, with H atoms omitted for clarity.

**Table 1.** Selected Bond Lengths (Å) and Angles (deg) for compound **4a**<sup>a</sup>

Mo(1)–Mo(2)	2.763(1)	Mo(2)–C(15)	2.382(5)
Mo(1)–P(1)	2.379(1)	Mo(2)–C(16)	2.451(4)
Mo(2)–P(1)	2.460(2)	Mo(2)–C(17)	2.454(4)
Mo(1)–O(3)	1.983(3)	Mo(2)–C(18)	2.359(4)
Mo(2)–O(3)	1.929(3)	Mo(1)–C(9)	2.446(5)
Mo(2)–O(4)	1.702(3)	Mo(1)–C(10)	2.427(6)
Mo(1)–N(1)	1.756(3)	Mo(1)–C(11)	2.353(6)
Re(1)–N(1)	1.985(3)	Mo(1)–C(12)	2.327(6)
Mo(2)–C(14)	2.356(4)	Mo(1)–C(13)	2.365(6)
Mo(1)–Ct(1)	2.090(6)	Mo(2)–Ct(2)	2.080(4)
Re(1)–Ct(3)	1.974(5)		
Mo(1)–P(1)–Mo(2)	69.63(5)	O(4)–Mo(2)–P(1)	99.1(1)
Mo(1)–O(3)–Mo(2)	89.9(1)	O(4)–Mo(2)–O(3)	105.4(2)
Mo(1)–Mo(2)–O(4)	112.8(1)	N(1)–Mo(1)–P(1)	93.7(1)
Mo(2)–Mo(1)–N(1)	99.4(1)	N(1)–Mo(1)–O(3)	102.1(1)
Mo(1)–N(1)–Re(1)	165.2(2)	N(1)–Re(1)–C(1)	93.5(2)
		C(1)–Re(1)–C(2)	88.6(2)
Mo(1)–Ct(1)–C(9)	93.3(1)	Mo(2)–Ct(2)–C(14)	87.5(1)
Mo(1)–Ct(1)–C(10)	91.4(1)	Mo(2)–Ct(2)–C(15)	88.8(1)
Mo(1)–Ct(1)–C(11)	88.5(1)	Mo(2)–Ct(2)–C(16)	93.0(1)
Mo(1)–Ct(1)–C(12)	87.5(2)	Mo(2)–Ct(2)–C(17)	93.0(1)
Mo(1)–Ct(1)–C(14)	89.1(3)	Mo(2)–Ct(2)–C(18)	87.7(1)

<sup>a</sup> Ct are the centroids of the cyclopentadienyl rings.

viewed as made of two cyclopentadienylmolybdenum fragments arranged in a transoid conformation and bridged by diphenylphosphide and oxo ligands. Each metal atom carries out one further ligand, a terminal oxygen atom on Mo(2), and a nitride ligand acting as an essentially linear bridge between Mo(1) and the  $\text{ReCp}'(\text{CO})_2$  fragment ( $\text{Re}–\text{N}–\text{Mo} = 165.2(2)^\circ$ ). The internal parameters in the latter fragment are unremarkable. As for the dimolybdenum center, we note a significant asymmetry in the bridges, with the  $\text{P}–\text{Mo}$  lengths differing by about 0.1 Å (closer to Mo(1)), this being only partially counterbalanced by the asymmetric positioning of the O(3) atom (ca. 0.05 Å closer to Mo(2)). The average  $\text{Mo}–\text{O}(3)$  length of about 1.95 Å is comparable to the  $\text{Mo}–\text{O}$  bond lengths measured in related compounds having angular oxygen bridges, such as

(15) Henrick, K.; McPartlin, M.; Horton, A. D.; Mays, M. J. *J. Chem. Soc., Dalton Trans.* **1988**, 1083.

(16) James, T. A.; McCleverty, J. A. *J. Chem. Soc. (A)* **1970**, 850.

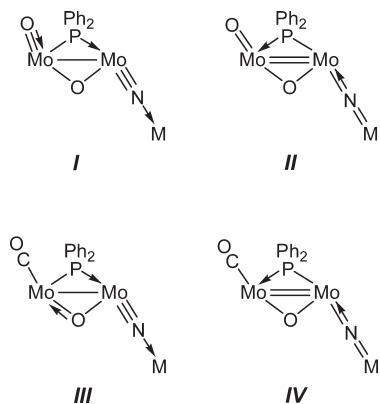


**Figure 2.** Canonical forms describing the metal–ligand and metal–metal bonding in compounds **4** and **3** (see text).

$[\text{Mo}_2\text{Cp}_2(\mu\text{-O})(\text{O})_2\{\mu\text{-C}_2(\text{CO}_2\text{Me})_2\}]^{17\text{a}}$  and  $[\text{Mo}_2\text{Cp}'_2(\mu\text{-NPh})(\mu\text{-O})(\text{O})_2]^{17\text{b}}$ . On the other hand, the terminal oxo ligand exhibits a much shorter Mo(2)–O(4) length of 1.702(3) Å, as usually found in organomolybdenum complexes having terminal oxo ligands, this being indicative of substantial multiplicity in the corresponding Mo–O bonds.<sup>18</sup> Concerning the nitride ligand, the Mo–N and N–Re lengths of 1.756(3) Å and 1.985(3) Å, respectively, are comparable to the corresponding values recently reported by us for the dimetallic nitride-bridged complex  $[\text{WReCpCp}'(\mu\text{-N})(\text{CO})_3\{\text{P}(\text{OMe})_3\}]$  (W–N = 1.81(3) Å, N–Re = 1.97(3) Å).<sup>12</sup> As we noted then, these figures can be considered respectively as slightly longer and significantly shorter than the reference values for triple Mo≡N and single Re–N bonds, respectively, and this suggests some delocalization of the  $\pi$ -interaction along the Mo–N–Re framework. Actually, the structural parameters of **4a** can be justified using a combination of two canonical forms (*I* and *II* in Figure 2) that imply this delocalization. This view is also substantiated by DFT calculations on **3b** to be discussed later on.

According to the EAN formalism, a Mo–Mo double bond might be formulated for compound **4a**, if we were to consider the terminal oxygen atom as a two-electron donor, but as a single bond if we consider it as a four-electron donor (forms *II* and *I* in Figure 2, respectively). Indeed the Mo–Mo length in this compound (2.763(1) Å) is much shorter than the reference single-bond figures usually measured for comparable structures (above ca. 2.9 Å), but still is somewhat longer than the reference values for related species having double Mo=Mo bonds, such as  $[\text{Mo}_2\text{Cp}_2(\mu\text{-N}=\text{CHPh})(\mu\text{-PCy}_2)(\text{CO})_2]$ , (2.632(1) Å),<sup>19\text{a}}  $[\text{Mo}_2\text{Cp}_2(\mu\text{-PCy}_2)(\mu\text{-CCO}_2\text{Me})(\text{CO})_2]$  (2.656(1) Å),<sup>19\text{b}} and  $[\text{Mo}_2\text{Cp}_2(\mu\text{-PPh}_2)_2(\text{CO})_2]$  (2.716(1) Å).<sup>20</sup> We can interpret this elongation as an indication that the oxo ligand might be using at a significant extent an additional electron pair for binding to the metal. Such additional interaction, in its extreme form, would make the oxo</sup></sup>

ligand to effectively behave as a four-electron donor atom, with this eventually leading to the formulation of a single Mo–Mo bond according to the EAN formalism (form *I* in Figure 2). However, we note that the elongation effect of the terminal oxo ligand on the metal–metal bond in **4a** seems to be substantially smaller than that previously found for related cyclopentadienyl oxo complexes such as  $[\text{Mo}_2\text{Cp}_2(\mu\text{-PPh}_2)(\mu\text{-CHCHPh})(\text{O})(\text{CO})]$ ,<sup>21\text{a}}  $[\text{Mo}_2\text{Cp}_2(\mu\text{-PPh}_2)_2(\text{O})(\text{CO})]$ ,<sup>20</sup> and  $[\text{W}_2\text{Cp}_2(\mu\text{-PPh}_2)(\mu\text{-CH}_2\text{PPh}_2)(\text{O})(\text{CO})]$ ,<sup>21\text{b}} which exhibit intermetallic distances in the range 2.89–2.95 Å. Therefore we conclude that the contribution of the canonical form *I* to the actual electronic structure of **4a** must be significant but not dominant, in agreement with the spectroscopic data in solution to be discussed later on.</sup></sup>

A further structural effect of the terminal oxo ligand can be finally appreciated in the cyclopentadienyl ligand bound to the same metal atom, since the carbon atoms positioned in *trans* with respect to the O(4) atom (C(16) and C(17)) exhibit Mo–C lengths about 0.1 Å longer than the other atoms of the ring (Table 1). This *trans* influence of terminal oxo ligands on cyclopentadienyl groups has been recognized previously,<sup>20,22</sup> and a similar *trans* influence might be expected for the nitride ligand, since the latter is also a strongly  $\pi$ -donor group. Indeed, the carbon atoms positioned in *trans* with respect to the N atom (C(9) and C(10)) are similarly distorted, with the corresponding Mo–C lengths being about 0.1 Å longer than those involving the other atoms of the ring. This distortion can be also measured in each case through the angles defined by the metal, centroid of the ring and the corresponding carbon atoms, these yielding values of about 93° for the C(9), C(10), C(16), and C(17) atoms (Table 1).

#### Spectroscopy and Solution Structure of Compounds **4**.

The IR spectrum of **4a**, when recorded in a KBr pellet, is consistent with the crystal structure just discussed and provides spectroscopic evidence for the presence of the oxo and nitride ligands, a piece of information also useful for the spectroscopic characterization of compounds **2** and **3**. Thus, in addition to the C–O stretching bands at 1904 and 1844  $\text{cm}^{-1}$  arising from the  $\text{Re}(\text{CO})_2$  fragment, this spectrum exhibits bands at 911, 897, and 837  $\text{cm}^{-1}$  that can be assigned to the stretches of the Mo≡N, Mo=O, and Mo–O–Mo moieties, respectively. In fact, the first band is very similar to those exhibited by the related nitride-bridged complexes  $[\text{MoReCpCp}'(\mu\text{-N})(\text{CO})_3\text{L}]$  (913 and 908  $\text{cm}^{-1}$  for L = CO and PPh<sub>3</sub>, respectively).<sup>12</sup> On the other hand, the bands at 897 and 837  $\text{cm}^{-1}$  are very close to the absorptions measured for related dimolybdenum complexes having both terminal and angular-bridging oxygen atoms, for instance  $[\text{Mo}_2\text{Cp}_2(\mu\text{-O})(\text{O})_2\{\mu\text{-C}_2(\text{CO}_2\text{Me})_2\}]$  (894 and 799  $\text{cm}^{-1}$ ),<sup>17\text{a}} and  $[\text{Mo}_2\text{Cp}'_2(\mu\text{-NPh})(\mu\text{-O})(\text{O})_2]$  (885 and 823  $\text{cm}^{-1}$ ).<sup>17\text{b}}</sup></sup>

Spectroscopic data for compounds **4a** and **4b**, both in the solid state and in solution (Table 2 and Experimental Section) are very similar to each other, thus indicating

(17) (a) Stichbury, J. C.; Mays, M. J.; Raithby, P. R.; Rennie, M.; Fullalove, M. R. *J. Chem. Soc., Chem. Commun.* **1995**, 1269. (b) Fletcher, J.; Hogarth, G.; Tocher, D. A. *J. Organomet. Chem.* **1991**, 403, 345.

(18) Bottomley, F.; Sutin, L. *Adv. Organomet. Chem.* **1988**, 28, 339.

(19) (a) Alvarez, M. A.; García, M. E.; Ramos, A.; Ruiz, M. A. *Organometallics* **2007**, 26, 1461. (b) García, M. E.; García-Vivó, D.; Ruiz, M. A. *Organometallics* **2008**, 27, 543.

(20) Adatia, T.; McPartlin, M.; Mays, M. J.; Morris, M. J.; Raithby, P. R. *J. Chem. Soc., Dalton Trans.* **1989**, 1555.

(21) (a) Endrich, K.; Korswagen, R.; Zhan, T.; Ziegler, M. L. *Angew. Chem., Int. Ed. Engl.* **1982**, 21, 919. (b) Alvarez, M. A.; García, M. E.; Riera, V.; Ruiz, M. A.; Falvello, L. R.; Bois, C. *Organometallics* **1997**, 16, 354.

(22) (a) Riera, V.; Ruiz, M. A.; Villafaña, F.; Bois, C.; Jeannin, Y. *Organometallics* **1993**, 12, 124. (b) Herrmann, W. A.; Herdtweck, E.; Flöel, M.; Kulpe, J.; Küsthardt, U.; Okuda, J. *Polyhedron* **1987**, 6, 1165.

Table 2. Selected IR and  $^{31}\text{P}\{\text{H}\}$  NMR Data for New Compounds

compound	$\nu(\text{CO})^a$	$\nu(\text{Mo}\equiv\text{N})^b$	$\nu(\text{Mo}=\text{O})^b$	$\nu(\text{MoOMo})^b$	$\delta(\text{P})^c$
$[\text{Mo}_2\text{ReCp}_2\text{Cp}'(\mu\text{-N})(\mu\text{-O})(\mu\text{-PPh}_2)(\text{CO})_4]$ ( <b>2a</b> )	1974 (s), 1901 (vs), 1836 (s)	918		813	204.4 <sup>d</sup>
$[\text{Mo}_2\text{ReCp}_2\text{Cp}'(\mu\text{-N})(\mu\text{-O})(\mu\text{-PPh}_2)(\text{CO})_3]$ ( <b>3a</b> )	1948 (m), 1896 (vs), 1832 (s)	912		805	169.2
$[\text{Mo}_2\text{Mn Cp}_2\text{Cp}'(\mu\text{-N})(\mu\text{-O})(\mu\text{-PPh}_2)(\text{CO})_3]$ ( <b>3b</b> )	1953 (m), 1912 (vs), 1854 (s)	910		808	169.1
$[\text{Mo}_2\text{ReCp}_2\text{Cp}'(\mu\text{-N})(\mu\text{-O})(\mu\text{-PPh}_2)(\text{O})(\text{CO})_2]$ ( <b>4a</b> )	1909 (vs), 1846 (s)	911	897	837	167.3
$[\text{Mo}_2\text{Mn Cp}_2\text{Cp}'(\mu\text{-N})(\mu\text{-O})(\mu\text{-PPh}_2)(\text{O})(\text{CO})_2]$ ( <b>4b</b> )	1926 (vs), 1869 (s)	925	894	840	168.3
$[\text{Mo}_2\text{Cp}_2(\mu\text{-PPh}_2)(\text{CN}'\text{Bu})(\text{CO})_2(\text{NO})]$ ( <b>5</b> )	2116 (m), <sup>e</sup> 1898 (vs), 1819 (s), 1605 (s) <sup>f</sup>				204.9
$[\text{Mo}_2\text{Cp}_2(\mu\text{-PPh}_2)(\mu\text{-}\eta^1\text{-}\eta^2\text{-CN}'\text{Bu})(\text{CO})(\text{NO})]$ ( <b>6</b> )	1858 (vs), 1647 (w), <sup>e</sup> 1604 (s) <sup>f</sup>				195.3

<sup>a</sup> Recorded in dichloromethane solution, unless otherwise stated;  $\nu$  in  $\text{cm}^{-1}$ . <sup>b</sup> Data recorded in KBr discs. <sup>c</sup> Recorded at 121.50 MHz in  $\text{CD}_2\text{Cl}_2$  solutions at 290 K unless otherwise stated,  $\delta$  in ppm relative to external 85% aqueous  $\text{H}_3\text{PO}_4$ . <sup>d</sup> Recorded at 253 K. <sup>e</sup>  $\nu(\text{CN})$ . <sup>f</sup>  $\nu(\text{NO})$ .

that both compounds share the same structure, and they are also consistent with the structure found in the crystal for **4a**. Both compounds display two C–O stretching bands with relative intensities (very strong and strong, respectively, in order of decreasing frequencies) indicative of the presence in each case of a  $\text{M}(\text{CO})_2$  oscillator with a C–M–C angle slightly below 90 degrees (cf. 88.6(2)<sup>o</sup> for **4a** in the crystal), while their wavenumbers are higher for the manganese compound as usual.<sup>23</sup> The presence of two different bridges connecting the Mo atoms removes any symmetry element from the molecule, and this is reflected in the appearance of two different carbonyl resonances and up to four resonances for the CH(Cp') groups in the  $^{13}\text{C}$  and  $^1\text{H}$  NMR spectra (see Experimental Section), which of course also exhibit two distinct Cp resonances in each case.

**Structural Characterization of Compounds 2 and 3.** The structure proposed for the tricarbonyl compounds **3a,b** is based on that determined for **4a** after replacement in the latter of the terminal oxo ligand with CO, and proved to be a true minimum in the potential energy surface of **3b**, as computed using DFT methods (see later). In fact, we trust that the transoid arrangement of the Cp ligands around the dimolybdenum center, usually more favored on steric grounds, is retained all the way from the initial tetracarbonyl compound **2** down to the dicarbonyls **4**. The presence in compounds **3** of a carbonyl ligand terminally bound to molybdenum is denoted by the observation of an additional C–O stretching band at about  $1950\text{ cm}^{-1}$  in the corresponding IR spectra (in addition to the characteristic bands due to the  $\text{M}(\text{CO})_2\text{Cp}'$  fragments) and also by the appearance of an additional NMR resonance ( $\delta$  240.0 ppm) in the  $^{13}\text{C}$  NMR spectrum of **3a**, substantially more deshielded than the resonances of the Re-bound carbonyls ( $\delta$  207.3, 206.5 ppm), and exhibiting a significant coupling to the  $^{31}\text{P}$  nucleus (18 Hz). Finally, the presence of the nitride ligand is denoted by the appearance in the corresponding solid-state IR spectra of the characteristic band at about  $910\text{ cm}^{-1}$ , while the absence of additional bands in this region, coupled to the presence of a band at about  $805\text{ cm}^{-1}$ , both support the presence in compounds **3** of a bridging, rather than terminal, oxo ligand.

The solid-state IR spectrum of **2a** also displays bands arising from nitride ( $918\text{ cm}^{-1}$ ) and oxo ( $813\text{ cm}^{-1}$ ) bridging ligands. The presence of an extra terminal CO ligand bound to molybdenum (compared to the tricarbonyl

compounds **3**) is not immediately obvious in the IR spectrum, which exhibits just three C–O stretching bands, but is clearly denoted by the appearance of two deshielded resonances (apart from those of the Re-bound carbonyls) in the carbonyl region of the  $^{13}\text{C}$  NMR spectrum. The very different P–C coupling of these two resonances (27 and ca. 0 Hz) indicates that both carbonyls must be bound to the same metal atom, since this would then lead to very different C–Mo–P angles for these two ligands, a critical structural factor governing the magnitude of two-bond P–C couplings.<sup>24</sup> Besides this, we note that a similar pattern in the P–C couplings is usually observed for the  $^{13}\text{C}$  resonances of the binuclear complexes of type  $[\text{Mo}_2\text{Cp}_2(\mu\text{-H})(\mu\text{-PRR}')(\text{CO})_4]$ , which locally exhibit comparable  $\text{CpMo}(\text{CO})_2$  fragments connected by PRR' and hydride bridges.<sup>25</sup> Incidentally, we note that the observed P–C coupling for the Mo-bound carbonyl in **3a** (18 Hz) is intermediate between the values observed for **2a**, in agreement with the proposed structures, implying C–Mo–P angles in the order **2a** (*cis* to P) < **3a** < **2a** (*trans* to P).

According to the EAN formalism, the tetracarbonyl compound **2a** has an electron-precise (34-electron) dimolybdenum center, and a single Mo–Mo bond must be formulated for this molecule. In contrast, the tricarbonyl compounds **3a,b** have two fewer electrons and a Mo–Mo double bond might be formulated for them, if we were to consider the bridging oxygen atom as a two-electron donor (as we do for **2a**). We have noted previously that 32-electron dimolybdenum compounds of the type *trans*- $[\text{Mo}_2\text{Cp}_2(\mu\text{-PRR}')(\mu\text{-X})(\text{CO})_2]$  (X = 3 electron-donor group) systematically exhibit  $^{31}\text{P}$  chemical shifts much lower than the corresponding electron-precise complexes  $[\text{Mo}_2\text{Cp}_2(\mu\text{-PRR}')(\mu\text{-H})(\text{CO})_4]$  or  $[\text{Mo}_2\text{Cp}_2(\mu\text{-PRR}')(\mu\text{-X})(\text{CO})_3]$ .<sup>25a,26</sup> The  $^{31}\text{P}$  shifts in compounds **2a** and **3** seems to follow this trend, with the resonances for the unsaturated tricarbonyls (ca. 169 ppm) being some 35 ppm more shielded than those of the electron-precise tetracarbonyl **2a** (204.4 ppm). Yet all these values

(24) (a) Jameson, C. J. In *Phosphorous-31 NMR Spectroscopy in Stereochemical Analysis*; Verkade, J. G., Quin, L. D., Eds.; VCH: New York, 1987; Chapter 6. (b) Wrackmeyer, B.; Alt, H. G.; Maisel, H. E. *J. Organomet. Chem.* **1990**, 399, 125.

(25) (a) García, M. E.; Riera, V.; Ruiz, M. A.; Rueda, M. T.; Sáez, D. *Organometallics* **2002**, 21, 5515. (b) Alvarez, C. M.; Alvarez, M. A.; García-Vivo, D.; García, M. E.; Ruiz, M. A.; Sáez, D.; Falvello, L. R.; Soler, T.; Herson, P. *Dalton. Trans.* **2004**, 4168. (c) Alvarez, C. M.; Alvarez, M. A.; Alonso, M.; García, M. E.; Rueda, M. T.; Ruiz, M. A. *Inorg. Chem.* **2006**, 45, 9593.

(26) (a) García, M. E.; García-Vivó, D.; Ruiz, M. A.; Aullón, G.; Alvarez, S. *Organometallics* **2007**, 26, 5912. (b) Alvarez, M. A.; García, M. E.; Ramos, A.; Ruiz, M. A.; Lanfranchi, M.; Tiripicchio, A. *Organometallics* **2007**, 26, 5454.

(23) Braterman, P. S. *Metal Carbonyl Spectra*; Academic Press: London, U. K., 1975.

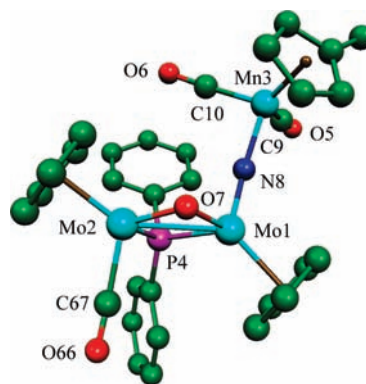
are substantially higher than those of comparable carbonyl compounds (cf. 135.3 and 180.9 ppm for *trans*-[Mo<sub>2</sub>Cp<sub>2</sub>(μ-PPh<sub>2</sub>)(μ-Cl)(CO)<sub>2</sub>]<sup>13</sup> and [Mo<sub>2</sub>Cp<sub>2</sub>(μ-PPh<sub>2</sub>)(μ-H)(CO)<sub>4</sub>]<sup>27</sup>, respectively). We attribute this deshielding effect in compounds **2** and **3** to the presence of the strongly π-donor nitride ligand on one of the molybdenum atoms. Perhaps the bridging oxo ligand in **3** also contributes to this effect. In fact, the terminal oxo ligands (which are strong π-donor groups) have been previously found to induce even stronger deshielding effects of about 100 ppm, as found in the pairs [Mo<sub>2</sub>Cp<sub>2</sub>(μ-PPh<sub>2</sub>)(μ-X)(CO)<sub>2</sub>]/[Mo<sub>2</sub>Cp<sub>2</sub>(μ-PPh<sub>2</sub>)(μ-X)(O)(CO)] (X = PPh<sub>2</sub>,<sup>20</sup> CH<sub>2</sub>PPh<sub>2</sub>).<sup>28</sup> In the case of the terminal oxo ligand, we can interpret this deshielding effect as associated with strong O→Mo π-interactions, which makes the O atom an effective donor of more than two electrons, thus reducing the intermetallic bond order, as discussed above for the oxocomplex **4a** (represented by the canonical form *I* in Figure 2). In the case of the tricarbonyls **3**, our DFT calculations on **3b**, to be discussed below, have revealed that the bridging oxygen atom is also involved in a similar π-bonding interaction with the dimetal center, this also leading to a reduction of the Mo–Mo bond order. The bonding in these tricarbonyl complexes thus might be analogously represented by two extreme canonical forms (*III* and *IV* in Figure 2) implying Mo–Mo and Mo–O bonds orders intermediate between 1 and 2.

**DFT Studies on the Tricarbonyl Complex 3b.** To better understand the nature of the Mo–Mo, Mo–O, and Mo–N bonding in the oxonitride complexes **2–4** we carried out DFT<sup>29</sup> calculations on the manganese compound **3b** (see the Experimental Section for details). The electronic structure and bonding in this unsaturated molecule has been analyzed through the properties of the relevant molecular orbitals, and also by inspection of the topological properties of the electron density, as managed in the AIM theory.<sup>30</sup>

The most relevant parameters derived from the geometry optimization of compound **3b** can be found in the Table 3, with the corresponding view being collected in the Figure 3. The structure is comparable to that of the dioxocomplex **4a**, if we replace the terminal oxo ligand in the latter by a carbonyl ligand, and many of the optimized bond lengths are comparable to those experimentally measured for **4a**, after allowing for the fact that the values calculated for lengths involving the metal atoms with the functionals currently used in the DFT computations of transition metal compounds tend to be slightly longer (less than 0.05 Å) than the corresponding experimental data.<sup>29a,31</sup> As expected for an unsaturated molecule, a relatively short intermetallic length (2.840 Å) is computed for **3a**, slightly longer than the experimental distance in

**Table 3.** Selected DFT-Optimized Bond Lengths and Angles for Compound **3b**

Mo(1)–Mo(2)	2.840	Mo(2)–C(67)	2.002
Mo(1)–O(7)	2.021	Mo(1)–N(8)	1.718
Mo(2)–O(7)	1.866	N(8)–Mn(3)	1.881
Mo(1)–P(4)	2.474	Mn(3)–C(10)	1.783
Mo(2)–P(4)	2.463	Mn(3)–C(9)	1.777
Mo(1)–O(7)–Mo(2)	93.8	Mo(2)–Mo(1)–N(8)	104.7
Mo(1)–P(4)–Mo(2)	70.2	Mo(1)–N(8)–Mn(3)	168.4
C(67)–Mo(2)–Mo(1)	97.7	C(10)–Mn(3)–C(9)	94.8
C(67)–Mo(2)–Mo(1)–N(8)	168.3		

**Figure 3.** DFT-optimized geometry for compound **3b**, with hydrogen atoms omitted for clarity.

the dioxocomplex **3a** (2.763(1) Å). This distance is about 0.1 Å longer than the intermetallic lengths computed at the same level of theory for the 32-electron carbyne complexes [Mo<sub>2</sub>Cp<sub>2</sub>(μ-COMe)(μ-PCy<sub>2</sub>)(CO)<sub>2</sub>] (2.734 Å) and [Mo<sub>2</sub>Cp<sub>2</sub>{μ-C(CO<sub>2</sub>Me)}(μ-PCy<sub>2</sub>)(CO)<sub>2</sub>] (2.699 Å), but yet substantially shorter than the values computed for related electron-precise complexes displaying single Mo–Mo bonds (e.g., 3.158 Å for *cis*-[Mo<sub>2</sub>Cp<sub>2</sub>(μ-COMe)(μ-PCy<sub>2</sub>)(CO)<sub>3</sub>]).<sup>26a</sup> Thus the intermetallic separation for **3b** would be consistent with the presence of significant multiplicity in the Mo–Mo interaction. As for the Mo–N length, 1.718 Å, it is slightly shorter than the corresponding experimental distance in **4a** (1.756(3) Å), which is suggestive of a very strong interaction, close to the triple bond. Finally, and more surprising, even when the Mo–O lengths for the bridging ligand in **3b** are on average only marginally shorter than the experimental values in **4a** (1.944 vs 1.956(3) Å), they are quite different from each other, with the shorter Mo(2)–O(7) length of 1.866 Å being compatible with the presence of substantial multiplicity in that bond, in agreement with the orbital analysis shown below.

The most relevant molecular orbitals of compound **3b** are depicted in the Figure 4, along with their associated energy and prevalent bonding character. Although there is extensive orbital mixing, we can appreciate that the HOMO (MO 155) has π Mo–N character (also present in MO 139), while the orthogonal component of the triple Mo–N bond is mainly represented by MO 138. Note that the latter has a significant participation of a Mn d orbital, thus giving support to the delocalization of the π Mo–N bonding along the Mo–N–Mn path, as proposed on the basis of the structural data and well represented by the canonical forms *III* and *IV* in Figure 2. Incidentally, we note that a similar delocalization is present in the

(27) Henrick, K.; McPartlin, M.; Horton, A. D.; Mays, M. J. *J. Chem. Soc., Dalton Trans.* **1988**, 1083.

(28) Garcia, G.; Garcia, M. E.; Melón, S.; Riera, V.; Ruiz, M. A.; Villafañe, F. *Organometallics* **1997**, *16*, 624.

(29) (a) Koch, W.; Holthausen, M. C. *A Chemist's Guide to Density Functional Theory*, 2nd ed.; Wiley-VCH: Weinheim, 2002. (b) Ziegler, T. *Chem. Rev.* **1991**, *91*, 651. (c) Foresman, J. B.; Frisch, ó. *Exploring Chemistry with Electronic Structure Methods*, 2nd ed.; Gaussian, Inc.: Pittsburg, 1996.

(30) (a) Bader, R. F. W. *Atoms in molecules—A Quantum Theory*; Oxford University Press: Oxford, U.K., 1990.

(31) Cramer, C. J. *Essentials of Computational Chemistry*, 2nd ed.; Wiley: Chichester, U.K., 2004.

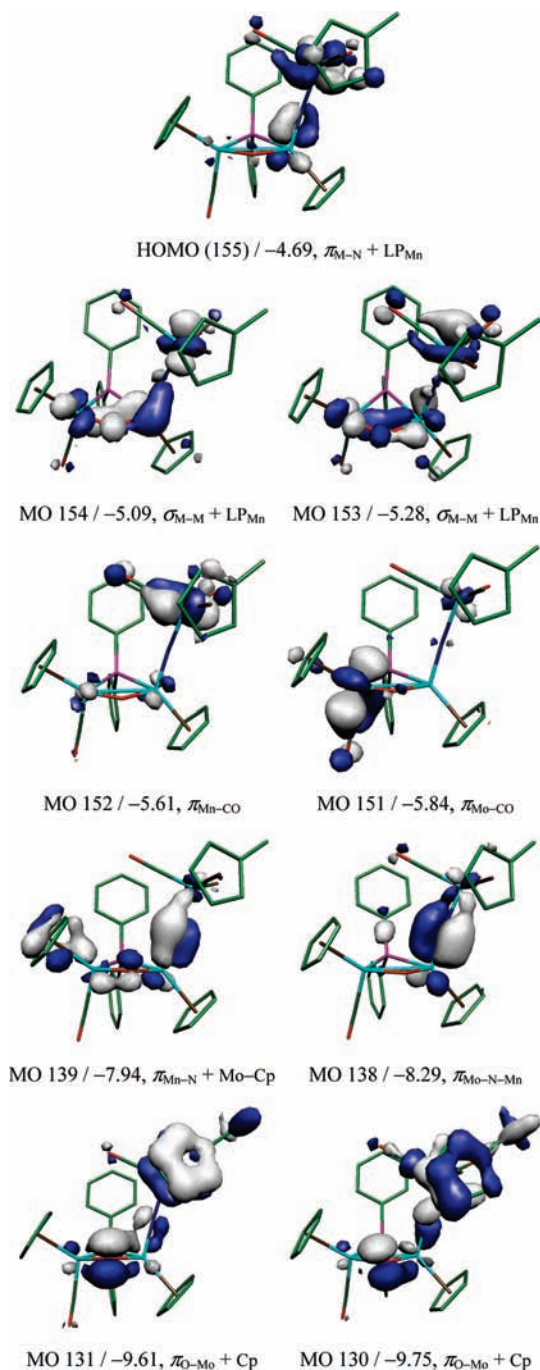


**Figure 4.** Selected molecular orbitals of compound **3b**, with their energies and main bonding character indicated below.

nitride-bridged complexes  $[\text{MM}'\text{CpCp}'(\mu\text{-N})(\text{CO})_3\text{L}]$  mentioned above.<sup>12</sup> The intermetallic interaction in **3b** is mainly described by MO 154 and MO 153, which represent an essentially  $\sigma_{\text{Mo-Mo}}$  bond mixed with a non-bonding electron pair on manganese. Interestingly, at energies between those of the  $\sigma_{\text{Mo-N}}$  and  $\sigma_{\text{Mo-O}}$  bonds, there are two orbitals (MO 131 and MO 130) representing a  $\pi$ -donor interaction from the O atom to the Mo atoms, this having the same phase as the  $\pi$ -bonding component of the intermetallic bond in this sort of bioctahedral molecules, and therefore being destructive in that respect. Thus we can say on a qualitative basis that upon the strengthening of this  $\pi$ -donor interaction of the bridging

**Table 4.** Topological Properties of the Electron Density at the Bond Critical Points in Compound **3b**<sup>a</sup>

bond	$\rho$	$\nabla^2\rho$
Mo(2)–O(7)	1.121	17.14
Mo(1)–O(7)	0.738	12.72
Mo(2)–C(67)	0.820	10.10
Mo(1)–N(8)	1.660	18.18
Mn(3)–N(8)	0.767	13.15
Mo(1)–P(4)	0.507	2.84
Mo(2)–P(4)	0.512	3.10
Mn(3)–C(9)	1.020	13.58
Mn(3)–C(10)	1.017	12.70

<sup>a</sup> Values of the electron density at the bond critical points ( $\rho$ ) are given in  $\text{e } \text{\AA}^{-3}$ ; values of the laplacian of  $\rho$  at these points ( $\nabla^2\rho$ ) are given in  $\text{e } \text{\AA}^{-5}$ .

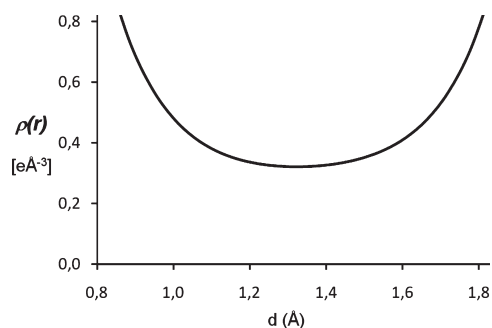


**Figure 5.** Electron density profile along the Mo(1)–Mo(2) vector for compound **3b**.

oxygen, then the intermetallic interaction gets closer to a single intermetallic bond. This is also well represented by the canonical forms *III* and *IV* in Figure 2, except that the MO picture does not easily account for the geometrical asymmetry of the oxygen bridge.

We have shown previously that the analysis of the electron density under the AIM theory provides valuable information (complementary to that of the MO analysis) for the characterization and even quantification of the bonds present in different unsaturated dimolybdenum complexes having carbyne, phosphide, and hydride bridges.<sup>26a,32,33</sup> We have therefore performed a similar analysis on **3b**, with special attention to the data relative to the metal–metal, metal–nitrogen, and metal–oxygen bonds. The values of electron density  $\rho$  and its Laplacian ( $\nabla^2\rho$ ) at the most relevant bond critical points (bcp) of these complexes are collected in Table 4.

We first note that we could not locate a Mo–Mo bcp even by using different basis for the Mo atoms. We have encountered this problem before for the mentioned 32-electron complexes  $[\text{Mo}_2\text{Cp}_2(\mu\text{-COR})(\mu\text{-PCy}_2)(\text{CO})_2]$ .<sup>26a</sup> An inspection of the values of  $\rho$  along the intermetallic vector reveals a relative flat plateau near the midpoint of the vector (Figure 5), where the mathematical conditions of the bcp cannot be satisfied. Even so, the minimum value of  $\rho$  is considerable,  $0.322 \text{ e } \text{\AA}^{-3}$ , actually a value intermediate between those computed for the above-mentioned carbyne complexes having a double Mo–Mo

(32) García, M. E.; García-Vivó, D.; Ruiz, M. A.; Aullón, G.; Alvarez, S. *Organometallics* **2007**, *26*, 4930.

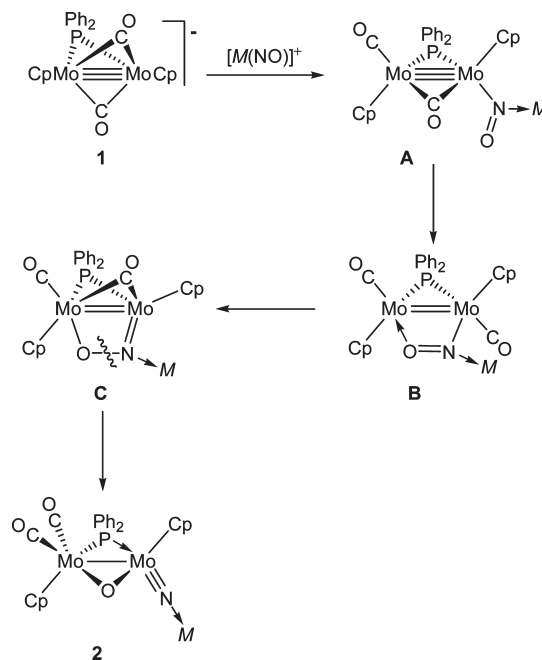
(33) García, M. E.; Ramos, A.; Ruiz, M. A.; Lanfranchi, M.; Marchio, L. *Organometallics* **2007**, *26*, 6197.

bond (ca.  $0.43 \text{ e } \text{\AA}^{-3}$ ), and those computed at the same level of theory for electron-precise complexes having single Mo–Mo bonds such as  $[\text{Mo}_2\text{Cp}_2(\mu\text{-COMe})(\mu\text{-PCy}_2)(\text{CO})_3]$  ( $0.22 \text{ e } \text{\AA}^{-3}$ ) and  $[\text{Mo}_2\text{Cp}_2(\text{CO})_6]$  ( $0.17 \text{ e } \text{\AA}^{-3}$ ].<sup>26a,32</sup> From these data, therefore, we conclude that there is also substantial multiplicity in the Mo–Mo bond of **3b**. Incidentally, we note that the minimum of  $\rho$  is reached at about  $1.33 \text{ \AA}$  from Mo(1), rather than at the exact midpoint of the vector ( $1.42 \text{ \AA}$ ). This can be justified by considering that the electron density at Mo(1) is lower (by ca.  $0.4 \text{ e}$ ) than that at the carbonyl-bearing Mo(2) atom (see Supporting Information).

As for the Mo–N and Mo–O bonds, although we have no data on related compounds to be used for comparative purposes, we note the very high value of  $\rho$  at the bcp of the Mo–N bond ( $1.660 \text{ e } \text{\AA}^{-3}$ ), consistent with its multiple character, and the noticeably higher value of  $\rho$  at the shorter O–Mo(2) bond ( $1.123 \text{ e } \text{\AA}^{-3}$ ), compared to that in the O–Mo(1) bond ( $0.738 \text{ e } \text{\AA}^{-3}$ ). Again we take these data as an independent indication of the  $\pi$ -interaction of the bridging oxygen atom with the Mo atom bearing the carbonyl ligand. As a result, we trust that the canonical forms *III* and *IV* depicted in Figure 2 give a simple but realistic description of the bonding in the tricarbonyl compounds **3**, where all the Mo–Mo, Mo–N, and Mo–O bonds seem to have intermediate bond orders, and the same can possibly be said of the canonical forms *I* and *II* for compounds **4**. In that case, we propose that the  $\pi$ -donor interaction will be arising from the terminal oxygen atom, rather than from the bridging one. Finally, in the case of the tetracarbonyl complexes **2**, we trust that the  $\pi$  interaction from the bridging oxygen atom is negligible, since now there is an additional carbonyl ligand, which is an excellent donor for a soft molybdenum atom.

**Pathways for N–O Bond Cleavage in the Reactions of Compound 1.** By following the results of our previous DFT calculation on the reactions of the anion  $[\text{WCp}(\text{CO})_3]^-$  with the nitrosyl cation  $[\text{MnCp}(\text{CO})_2(\text{NO})]^+$  we can reasonably assume that the formation of compounds **2** also proceeds under orbital control, and thus would be initiated by the nucleophilic attack of the anion to the nitrogen atom of the nitrosyl ligand in the cation, strongly involved in the corresponding lowest unoccupied molecular orbital (LUMO).<sup>12</sup> This most probably would involve a single Mo site of the anion for steric reasons, even when DFT calculations on the related anion  $[\text{Mo}_2\text{Cp}_2(\mu\text{-PCy}_2)(\mu\text{-CO})_2]^-$  indicate that the suitable donor orbitals involve both metal atoms.<sup>32</sup> The intermediate **A** thus formed (Scheme 2) has a nitrosyl ligand bridging the Re atom and a highly unsaturated dimolybdenum center, and then it would rearrange to reduce this electronic deficiency by coordinating its oxygen atom to the second Mo center. The resulting intermediate **B** would have a  $\mu_3$ -nitrosyl ligand in a very uncommon arrangement. Actually, to the best of our knowledge all known compounds having nitrosyl ligands bridging three metal atoms bind the metals exclusively

**Scheme 2.** Proposed Steps for the N–O Bond Cleavage Reactions of Compound **1** ( $M = \text{ReCp}'(\text{CO})_2$  or  $\text{MnCp}'(\text{CO})_2$ )



through the N atom. However, there are a few examples where a nitrosyl ligand has been found coordinated through both the N and O atoms, either to two ( $\mu_2\text{-N:O}$  mode)<sup>34</sup> or to four metal atoms ( $\mu_4\text{-N:O:N:O}$  and  $\mu_4\text{-N:N:N:O}$  modes).<sup>35,36</sup> Interestingly, in all these cases the N–O bond of the nitrosyl ligand is considerably elongated, thus suggesting a significant activation with respect to the full cleavage of this bond. In the case of intermediate **B**, the progressive weakening of the N–O bond might readily proceed first through a rearrangement rendering double N=Mo and single N–O bonds (**C** in Scheme 2) and finally by full cleavage of the latter bond, also involving the opening of the bridging carbonyl at some stage, to finally yield the observed tetracarbonyl product of type **2**. In our view, then, the great electronic and coordinative unsaturation of the anion **1** is a circumstance of critical influence for the successful cleavage of the N–O bond being observed, since this induces and/or facilitates the simultaneous coordination of both the N and O atoms of the nitrosyl ligand, as required for the cleavage of this ligand without direct participation of carbonyl ligands (i.e., processes yielding  $\text{CO}_2$ ).<sup>12</sup>

**Nitrosylation Reactions of Compound 1.** As stated above, we examined these reactions so as to check whether the electronic and coordinative unsaturation of this anionic complex would be enough to induce the cleavage of the nitrosyl ligand. The reaction of **1** with the strong nitrosylating agent  $(\text{NO})\text{BF}_4$  was difficult to control, and a mixture of several compounds was obtained under all experimental conditions examined. In contrast, the reaction of **1** with a milder reagent such as *N*-methyl-*N*-nitroso-*p*-toluenesulfonamide proceeds more

(34) (a) Legzdins, P.; Rettig, S. J.; Veltheer, J. E.; Batchelor, R. J.; Einstein, F. W. B. *Organometallics* **1993**, *12*, 3575. (b) Ipaktschi, J.; Mohseni-Ala, J.; Dülmer, A.; Steffens, S.; Wittenburg, C.; Heck, J. *Organometallics* **2004**, *23*, 4902.

(35) Beringhelli, T.; Ciani, G.; D'Alfonso, G.; Molinari, H.; Sironi, A.; Freni, M. *J. Chem. Soc., Chem. Commun.* **1984**, 1327.

(36) (a) Kyba, E. P.; Kashyap, R. P.; Mountzouris, J. A.; Davis, R. E. *J. Am. Chem. Soc.* **1990**, *112*, 905. (b) Ellis, D.; Farrugia, L. J. *J. Cluster Sci.* **2001**, *12*, 243.

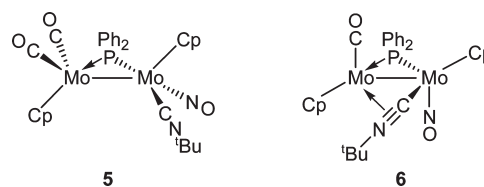


selectively to give the electron-precise nitrosyl derivative  $[\text{Mo}_2\text{Cp}_2(\mu\text{-PPh}_2)(\text{CO})_3(\text{NO})]$ . This complex has been previously prepared by us through the reaction of the paramagnetic complex  $[\text{Mo}_2\text{Cp}_2(\mu\text{-PPh}_2)(\text{CO})_4]$  with  $\text{NO}$ .<sup>14</sup> Since the observed product contains one more CO than the starting anion, it can be guessed that a very unstable unsaturated nitrosyl derivative is initially formed, this then evolving through spontaneous carbonylation rather than through any N–O bond cleavage process, as it will be discussed later on. We then attempted to modify this evolution by carrying out the nitrosylation reaction in the presence of  $\text{CN}^t\text{Bu}$ , a ligand comparable to CO, but with higher donor ability and steric demands, which perhaps would open a new  $\text{CO}_2$ -elimination channel for the cleavage of the nitrosyl ligand.<sup>12</sup> Indeed this reaction proceeds smoothly below room temperature, and the formation of the tricarbonyl complex  $[\text{Mo}_2\text{Cp}_2(\mu\text{-PPh}_2)(\text{CO})_3(\text{NO})]$  is essentially suppressed, but no cleavage of the nitrosyl ligand is induced either. Instead, a mixture of the isocyanide complexes  $[\text{Mo}_2\text{Cp}_2(\mu\text{-PPh}_2)(\text{CN}^t\text{Bu})(\text{CO})_2(\text{NO})]$  (**5**) and  $[\text{Mo}_2\text{Cp}_2(\mu\text{-PPh}_2)(\mu\text{-}\eta^1\text{:}\eta^2\text{-CN}^t\text{Bu})(\text{CO})(\text{NO})]$  (**6**) is obtained in an about 1:2 ratio (Chart 2). Although these products differ by just one CO ligand, separate experiments indicated that compound **6** does not react with CO under ordinary conditions, whereas compound **5** neither experiences spontaneous decarbonylation in solution, even in refluxing toluene. Thus, we must conclude that the formation of these two products follow from different reaction pathways, a matter to be discussed later on. We should finally stress that, in spite of the fact that compound **5** can be formally derived by replacement of CO with  $\text{CN}^t\text{Bu}$  in the tricarbonyl complex  $[\text{Mo}_2\text{Cp}_2(\mu\text{-PPh}_2)(\text{CO})_3(\text{NO})]$ , this substitution reaction actually does not take place even in refluxing toluene solution, as indicated by independent experiments.

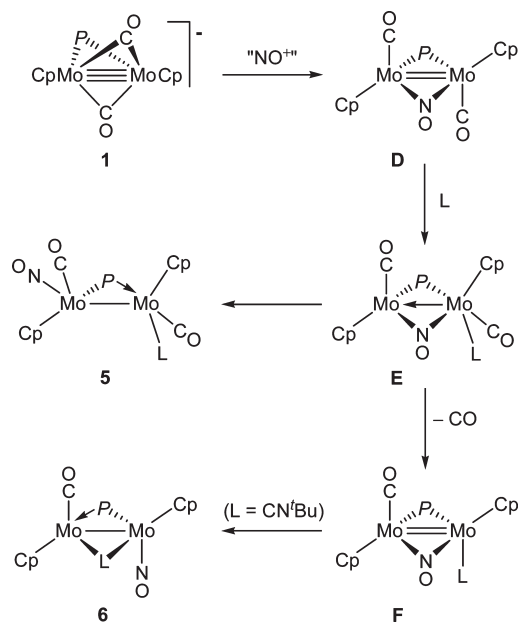
**Structural Characterization of Compounds 5 and 6.** The proposed structure of the dicarbonyl compound **5** is based on that crystallographically determined for the tricarbonyl complex  $[\text{Mo}_2\text{Cp}_2(\mu\text{-PPh}_2)(\text{CO})_3(\text{NO})]$ .<sup>14</sup> The presence of the four terminal ligands is immediately denoted by the appearance of four medium to strong bands in the characteristic regions of the C–N, C–O, and N–O bond stretches of the corresponding terminal ligands (Table 2), while the strong NMR deshielding of the P nucleus, similar to that of the tetracarbonyl complex **2a**, is fully consistent with the electron-precise nature of this molecule. Out of the possible arrangements of the terminal ligands, our proposal for **5** is derived from the P–C couplings exhibited by the <sup>13</sup>C NMR resonances of the carbonyl ( $\delta$  243.5 ppm,  $J_{\text{CP}} = 21$  Hz and  $\delta$  234.4 ppm,  $J_{\text{CP}} \sim 0$  Hz) and isocyanide ( $\delta$  169.7 ppm,  $J_{\text{CP}} \sim 0$  Hz) ligands, these denoting a positioning relative to the P atom *cis*, *trans*, and *trans*, respectively.

The IR spectrum of compound **6** exhibits strong bands at 1858 and 1604  $\text{cm}^{-1}$ , which are indicative of the presence of terminal CO and NO ligands, respectively. This spectrum shows no high-frequency band characteristic of terminal isocyanide ligands, but exhibits a weak and broadband at 1647  $\text{cm}^{-1}$  suggestive of the presence of a four-electron donor ( $\mu\text{-}\eta^1\text{:}\eta^2$ ) bridging isocyanide

Chart 2



**Scheme 3.** Pathways in the Nitrosylation Reactions of Compound **1** ( $P = \text{PPh}_2$ ;  $L = \text{CO}, \text{CN}^t\text{Bu}$ )



ligand, by comparison with the IR data of the related complexes  $[\text{Mo}_2\text{Cp}_2(\mu\text{-}\eta^1\text{:}\eta^2\text{-CN}^t\text{Bu})(\text{CO})_2(\mu\text{-dppm})]$  and  $[\text{Mo}_2\text{Cp}_2(\mu\text{-}\eta^1\text{:}\eta^2\text{-CN}^t\text{Bu})(\text{CO})_3(\kappa^1\text{-dppm})]$ .<sup>28,37</sup> This is further confirmed by the <sup>13</sup>C NMR spectrum of **6**, which exhibits an abnormally deshielded isocyanide resonance at 214.6 ppm, as found for the mentioned compounds and related dimolybdenum complexes having  $\mu\text{-}\eta^1\text{:}\eta^2$  isocyanide ligands.<sup>38</sup> Our spectroscopic data, however, do not allow us to define whether the carbon atoms of the isocyanide and carbonyl ligands in **6** are bound to the same or different metal atom, although the second possibility seems more likely on mechanistic grounds, next discussed. Our data do not either show whether the CpMo moieties in **6** are positioned in a *cisoid* or *transoid* arrangement, but the latter is the one most commonly found in this sort of cyclopentadienyl complexes, presumably favored over the *cisoid* isomers on steric grounds.

#### Pathways in the Nitrosylation Reaction of Compound **1**.

The nucleophilic attack of the unsaturated anion **1** on *N*-methyl-*N*-nitroso-*p*-toluenesulfonamide is expected to give initially an unsaturated nitrosyl-bridged derivative  $[\text{Mo}_2\text{Cp}_2(\mu\text{-NO})(\mu\text{-PPh}_2)(\text{CO})_2]$  (**D** in Scheme 3) much in the same way as the protonation reaction of **1** gives the corresponding hydride-bridged derivative  $[\text{Mo}_2\text{Cp}_2(\mu\text{-H})(\mu\text{-PPh}_2)(\text{CO})_2]$ .<sup>13</sup> Apparently, this intermediate

(37) Riera, V.; Ruiz, M. A.; Villafañe, F.; Bois, C.; Jeannin, Y. J. *Organomet. Chem.* **1990**, 382, 407.

(38) Adams, H.; Bailey, N. A.; Bannister, C.; Faers, M. A.; Fedorko, P.; Osborn, V. A.; Winter, M. J. *J. Chem. Soc., Dalton Trans.* **1987**, 341.

would be very unstable, and it would partially decompose, thus liberating CO that rapidly would react with undecomposed molecules to give the electron-precise and very stable tricarbonyl  $[\text{Mo}_2\text{Cp}_2(\mu\text{-PPh}_2)(\text{CO})_3(\text{NO})]$ . Decomposition of **D** is then expectedly avoided in the presence of isocyanide, since any ligand being present (L) would rapidly react with **D** to give an electron precise intermediate **E**, perhaps still retaining the nitrosyl bridge, if we use the results of the carbonylation reactions of the isoelectronic complexes  $[\text{Mo}_2\text{Cp}_2(\mu\text{-PCy}_2)(\mu\text{-X})(\text{CO})_2]$  (X = alkenyl, COMe) as a model.<sup>26</sup> The intermediate **E** would easily rearrange in different ways eventually opening the nitrosyl bridge, then leading to the dicarbonyl **5** or, when L = CO, to the tricarbonyl  $[\text{Mo}_2\text{Cp}_2(\mu\text{-PPh}_2)(\text{CO})_3(\text{NO})]$  as noted above. Alternatively, when L = CN<sup>t</sup>Bu the intermediate **E** might evolve through decarbonylation, perhaps induced by the presence on the same metal atom of the relatively bulky CN<sup>t</sup>Bu ligand, to give a new unsaturated intermediate **F**, which then would reach the electronic saturation by a rearrangement of the isocyanide ligand, from terminal to the  $\mu\text{-}\eta^1\text{:}\eta^2$  bridging mode, this being accompanied by a displacement of the bridging nitrosyl to a terminal position, thus explaining the formation of the isocyanide-bridged complex **6**.

**Concluding Remarks.** The formation of the nitride-bridged complexes **2** (which in turn are the precursors of the nitride-bridged compounds **3** and **4**) can be understood as derived initially from an orbitally controlled nucleophilic attack of a metal atom of the anion **1** to the N atom of the nitrosyl ligand in the cations  $[\text{MCp}'(\text{NO})(\text{CO})_2]^+$ . Because of the electronic and coordinative unsaturation of the resulting trimetallic intermediate, the system does not evolve through a CO<sub>2</sub> elimination pathway, as previously observed by us in the reactions of the electron-precise anions of type  $[\text{MCp}(\text{CO})_2\text{L}]^-$ , and this gives further support to our previous hypothesis that a close approach of the carbonyl ligands to the bridging nitrosyl ligand in the intermediates initially formed is essential for this particular reaction pathway to be operative. Instead, we trust that the unsaturated dimolybdenum center derived from **1** allows and induces the simultaneous coordination of both the N and O atoms of the nitrosyl ligand to partially relieve this deficiency, thus initiating a progressive weakening of the N–O bond in the nitrosyl ligand eventually leading to its full cleavage, to yield metal-bound nitride and oxo ligands and thus achieving the complete electronic saturation of the resulting molecule. The presence of a metal initially bound to the nitrosyl ligand is essential to the overall process, since otherwise this ligand binds the unsaturated dimolybdenum center in non-activated (with respect to the N–O bond cleavage) coordination modes involving only the nitrogen atom, as observed in the nitrosylation reactions of the anion **1**. Further work will be needed to prove the use of the above ideas for a better understanding of the ways in which transition-metal complexes can cleave the strong bond of the NO molecule, and for the design of polymeric substrates able to carry out this process in an efficient and even catalytic way.

## Experimental Section

**General Procedures and Starting Materials.** All manipulations and reactions were carried out under a nitrogen (99.995%)

atmosphere using standard Schlenk techniques. Solvents were purified according to literature procedures and distilled prior to their use.<sup>39</sup> Petroleum ether refers to that fraction distilling in the range 338–343 K. Compounds  $[\text{MCp}'(\text{CO})_2(\text{NO})]\text{BF}_4$  [M = Mn (**1**),<sup>40</sup> Re (**2**)<sup>41</sup>] and THF solutions of  $\text{Na}[\text{Mo}_2\text{Cp}_2(\mu\text{-PPh}_2)(\mu\text{-CO})_2]$  (**1**)<sup>13</sup> were prepared as described previously. Chromatographic separations were carried out on alumina using jacketed columns cooled by tap water (ca. 285 K) or by a closed 2-propanol circuit, kept at the desired temperature with a cryostat. For this purpose, commercial aluminum oxide (Aldrich, activity I, 150 mesh) was degassed under vacuum prior to use. The latter was mixed under nitrogen with the appropriate amount of water to reach the activity desired. All other reagents were obtained from the usual commercial suppliers and used as received. IR stretching frequencies were measured in solution or KBr discs. Nuclear Magnetic Resonance (NMR) spectra were routinely recorded at 300.13 (<sup>1</sup>H), 121.50 (<sup>31</sup>P{<sup>1</sup>H}), or 75.47 MHz (<sup>13</sup>C{<sup>1</sup>H}) at 290 K in CD<sub>2</sub>Cl<sub>2</sub> solutions unless otherwise is stated. Chemical shifts ( $\delta$ ) are given in ppm, relative to internal tetramethylsilane (<sup>1</sup>H, <sup>13</sup>C) or external 85% aqueous H<sub>3</sub>PO<sub>4</sub> (<sup>31</sup>P). Coupling constants (*J*) are given in hertz.

**Preparation of  $[\text{Mo}_2\text{ReCp}_2\text{Cp}'(\mu\text{-N})(\mu\text{-O})(\mu\text{-PPh}_2)(\text{CO})_4]$  (**2a**).** Solid  $[\text{ReCp}'(\text{CO})_2(\text{NO})]\text{BF}_4$  (0.075 g, 0.17 mmol) was added to a freshly prepared THF solution (10 mL) containing about 0.17 mmol of compound **1**, cooled at 193 K. The mixture turned into black-green instantaneously and was further stirred for 30 min while allowing it to warm up to 243 K, to yield an orange mixture. The solvent was then removed under vacuum, the residue was extracted with a minimum CH<sub>2</sub>Cl<sub>2</sub>, and the extract was chromatographed on alumina (activity 3.5) at 243 K. Elution with dichloromethane-petroleum ether (1:1) gave a minor orange fraction containing some  $[\text{Mo}_2(\mu\text{-PPh}_2)(\text{CO})_3(\text{NO})]$ . Elution with THF-petroleum ether (1:1) gave a major orange fraction which yielded, after removal of solvents under vacuum at 243 K, compound **2a** as a brown-orange powder (0.095 g, 62%). This compound is thermally unstable, and it transforms into **3a** above 253 K in dichloromethane solution. Thus satisfactory elemental analysis for this compound could not be obtained. <sup>1</sup>H NMR (400.13 MHz, 253 K):  $\delta$  8.3–6.7 (m, Ph, 10H), 5.50, 5.24 (2s, 2 × 5H, Cp), 5.11, 4.99, 4.94, 4.89 (4m, 4 × 1H, C<sub>5</sub>H<sub>4</sub>), 2.11 (s, 3H, Me). <sup>13</sup>C{<sup>1</sup>H} NMR (100.63 MHz, 253 K):  $\delta$  239.7 (d, *J*<sub>CP</sub> = 27, MoCO), 233.7 (s, MoCO), 206.5, 206.1 (2s, ReCO), 141.5 [d, *J*<sub>PC</sub> = 41, C<sup>1</sup>(Ph)], 136.5 [d, *J*<sub>PC</sub> = 49, C<sup>1</sup>(Ph)], 135.5–128.7 (m, Ph), 110.5 [s, C<sup>1</sup>(C<sub>5</sub>H<sub>4</sub>)], 105.2, 97.6 (2s, Cp), 83.5, 83.4, 83.1, 82.6 [4s, C<sup>2,3</sup>(C<sub>5</sub>H<sub>4</sub>)], 13.9 (s, Me).

**Preparation of  $[\text{Mo}_2\text{ReCp}_2\text{Cp}'(\mu\text{-N})(\mu\text{-O})(\mu\text{-PPh}_2)(\text{CO})_3]$  (**3a**).** A solution of compound **2a** (0.046 g, 0.05 mmol) in dichloromethane (20 mL) was stirred at room temperature for 2 h to give a dark green solution which was filtered through alumina (3 × 2.5 cm, activity 3.5) at 285 K. Addition of petroleum ether to the filtrate and removal of solvents under vacuum gave compound **3a** as an emerald-green, air-sensitive powder (0.039 g, 88%). Anal. Calcd for C<sub>31</sub>H<sub>27</sub>Mo<sub>2</sub>NO<sub>4</sub>PRe: C, 42.00; H, 3.07; N, 1.58. Found: C, 41.60; H, 3.25; N, 1.70. <sup>1</sup>H NMR (200.13 MHz):  $\delta$  8.2–6.5 (m, Ph, 10H), 6.05 (s, 5H, Cp), 5.59 (d, *J*<sub>PH</sub> = 1, 5H, Cp), 4.96, 4.68 (2m, 2 × 1H, C<sub>5</sub>H<sub>4</sub>), 4.75 (m, 2H, C<sub>5</sub>H<sub>4</sub>), 1.71 (s, 3H, Me). <sup>13</sup>C{<sup>1</sup>H} NMR (100.63 MHz, 253 K):  $\delta$  240.0 (d, *J*<sub>CP</sub> = 18, MoCO), 207.3, 206.5 (2s, ReCO), 144.1 [d, *J*<sub>PC</sub> = 28, C<sup>1</sup>(Ph)], 138.1 [d, *J*<sub>PC</sub> = 52, C<sup>1</sup>(Ph)], 135.8–128.5 (m, Ph), 110.3 [s, C<sup>1</sup>(C<sub>5</sub>H<sub>4</sub>)], 104.1, 99.4 (2s, Cp), 84.2, 84.1, 83.9, 81.6 [4s, C<sup>2,3</sup>(C<sub>5</sub>H<sub>4</sub>)], 14.0 (s, Me).

**Preparation of  $[\text{Mo}_2\text{MnCp}_2\text{Cp}'(\mu\text{-N})(\mu\text{-O})(\mu\text{-PPh}_2)(\text{CO})_3]$  (**3b**).** Solid  $[\text{MnCp}'(\text{CO})_2(\text{NO})]\text{BF}_4$  (0.052 g, 0.17 mmol) was added to a freshly prepared THF solution (10 mL) containing

(39) Armarego, W. L. F.; Chai, C. *Purification of Laboratory Chemicals*, 5th ed.; Butterworth-Heinemann: Oxford, U.K., 2003.

(40) Connelly, N. G. *Inorg. Synth.* **1974**, *15*, 91.

(41) Tam, W.; Liu, G. Y.; Wang, K. W.; Kiel, W. A.; Wong, V. K.; Gladysz, J. A. *J. Am. Chem. Soc.* **1982**, *104*, 141.

about 0.17 mmol of compound **1**, cooled at 193 K, and the mixture was further stirred for 3 h while allowing it to warm up to room temperature, to yield a brown-green mixture. The solvent was then removed under vacuum, the residue was extracted with a minimum dichloromethane-petroleum ether (1:1), and the extract was chromatographed on alumina (activity 3.5) at 285 K. Elution with the same solvent mixture gave a minor orange fraction containing some  $[\text{Mo}_2\text{Cp}_2(\mu\text{-PPh}_2)(\text{CO})_3(\text{NO})]$  and  $[\text{Mo}_2\text{Cp}_2(\mu\text{-H})(\mu\text{-PPh}_2)(\text{CO})_4]$  in similar amounts. Elution with dichloromethane-petroleum ether (1:1) gave a red-brown fraction containing  $[\text{Mn}_2\text{Cp}'_2(\text{CO})_2(\text{NO})_2]$  and minor amounts of other uncharacterized species. Finally, elution with dichloromethane gave a green fraction which yielded, after removal of solvents under vacuum, compound **3b** as a green, air-sensitive microcrystalline solid (0.033 g, 26%). Thus satisfactory elemental analysis for this compound could not be obtained.  $^1\text{H NMR}$ :  $\delta$  8.29–6.42 (m, Ph, 10H), 6.04, 5.57 (2s, 2  $\times$  5H, Cp), 4.19, 4.10 (2m, 2  $\times$  1H, C<sub>5</sub>H<sub>4</sub>), 3.99 (m, 2H, C<sub>5</sub>H<sub>4</sub>), 1.64 (s, 3H, Me).

**Preparation of  $[\text{Mo}_2\text{ReCp}_2\text{Cp}'(\mu\text{-N})(\mu\text{-O})(\mu\text{-PPh}_2)(\text{O})(\text{CO})_2]$  (**4a**).** A solution of compound **3a** (0.045 g, 0.05 mmol) in dichloromethane (12 mL) was stirred at room temperature in the presence of air for 30 min to give a blue solution which was chromatographed on alumina (10  $\times$  2.5 cm, activity 3.5) at 285 K. Elution with dichloromethane gave a dark blue fraction. Removal of solvents under vacuum and crystallization of the residue from dichloromethane-petroleum ether at 253 K gave compound **4a** as a blue microcrystalline solid (0.036 g, 82%). The crystals used in the X-ray study were grown by the slow diffusion at room temperature of a layer of diethyl ether into a concentrated solution of the complex in toluene. Anal. Calcd for C<sub>30</sub>H<sub>27</sub>Mo<sub>2</sub>NO<sub>4</sub>PRE: C, 41.20; H, 3.11; N, 1.60. Found: C, 41.09; H, 3.00; N, 1.75.  $^1\text{H NMR}$  (400.13 MHz):  $\delta$  8.18–7.28 (m, Ph, 10H), 5.68, 5.55 (2d,  $J_{\text{PH}} = 1, 2 \times 5\text{H}$ , Cp), 5.04, 5.01 (2m, 2  $\times$  2H, C<sub>5</sub>H<sub>4</sub>), 2.12 (s, 3H, Me).  $^{13}\text{C}\{^1\text{H}\}$  NMR (100.63 MHz, 213 K):  $\delta$  205.2, 205.0 (2s, ReCO), 137.5 [d,  $J_{\text{PC}} = 37$ , C<sup>1</sup>(Ph)], 135.7–128.3 [m, C<sup>1</sup>(Ph) and C<sup>2,3</sup>(Ph)], 109.9 [s, C<sup>1</sup>(C<sub>5</sub>H<sub>4</sub>)], 104.4, 102.4 (2s, Cp), 84.6, 84.5, 83.7, 83.3 [4s, C<sup>2,3</sup>(C<sub>5</sub>H<sub>4</sub>)], 13.2 (s, Me).

**Preparation of  $[\text{Mo}_2\text{MnCp}_2\text{Cp}'(\mu\text{-N})(\mu\text{-O})(\mu\text{-PPh}_2)(\text{O})(\text{CO})_2]$  (**4b**).** A solution of compound **3b** (0.030 g, 0.040 mmol) in dichloromethane (10 mL) was stirred at room temperature in the presence of air for 20 min to give a blue solution. Workup as described for **4a** yielded compound **4b** as a green-black microcrystalline solid (0.023 g, 78%). Anal. Calcd for C<sub>30</sub>H<sub>27</sub>MnMo<sub>2</sub>NO<sub>4</sub>P: C, 48.47; H, 3.66; N, 1.88. Found: C, 48.35; H, 3.48; N, 1.95.  $^1\text{H NMR}$ :  $\delta$  8.13–7.29 (m, Ph, 10H), 5.71, 5.53 (2s, 2  $\times$  5H, Cp), 4.52, 4.39, 4.32, 4.27 (4m, 4  $\times$  1H, C<sub>5</sub>H<sub>4</sub>), 1.82 (s, 3H, Me).

**Nitrosylation of Compound 1.** Solid *N*-methyl-*N*-nitroso-*p*-toluenesulfonamide (0.036 g, 0.17 mmol) and neat CN<sup>t</sup>Bu (20  $\mu\text{L}$ , 0.17 mmol) were added to a freshly prepared THF solution (10 mL) containing about 0.17 mmol of compound **1**, cooled at 203 K, and the mixture was further stirred for 90 min while allowing it to warm up to room temperature, to yield a brown-orange mixture. The solvent was then removed under vacuum, the residue was extracted with toluene (5 mL), and the extract was chromatographed on alumina (activity 3.5) at 285 K. Elution with toluene gave a rose-orange fraction. Removal of the solvent and crystallization of the residue from toluene-petroleum ether at 253 K gave compound  $[\text{Mo}_2\text{Cp}_2(\mu\text{-PPh}_2)(\text{CN}^t\text{Bu})(\text{CO})_2(\text{NO})]$  (**5**) as an orange powder (0.031 g, 27%). Elution with dichloromethane gave a yellow-orange fraction. Workup as above gave compound  $[\text{Mo}_2\text{Cp}_2(\mu\text{-PPh}_2)(\mu\text{-}\eta^1\text{-CN}^t\text{Bu})(\text{CO})(\text{NO})]$  (**6**) as a yellow powder (0.038 g, 35%). *Data for compound 5*: Anal. Calcd for C<sub>29</sub>H<sub>29</sub>Mo<sub>2</sub>N<sub>2</sub>O<sub>3</sub>P: C, 51.49; H, 4.32; N, 4.14. Found: C, 51.56; H, 4.49; N, 4.06.  $^1\text{H NMR}$  (200.13 MHz):  $\delta$  7.60–6.83 (m, Ph, 10H), 5.12, 4.96 (2s, 2  $\times$  5H, Cp), 1.70 (s, 9H, Me).  $^{13}\text{C}\{^1\text{H}\}$  NMR (50.33 MHz):  $\delta$  243.5 (d,  $J_{\text{CP}} = 21$ , MoCO), 234.4 (s, MoCO), 169.7 (s, MoCN), 147.0 [d,  $J_{\text{PC}} = 34$ , C<sup>1</sup>(Ph)], 142.6 [d,  $J_{\text{PC}} = 36$ , C<sup>1</sup>(Ph)], 135.2 [d,  $J_{\text{PC}} = 9$ ,

**Table 5.** Crystal Data for Compound **4a**

mol formula	C <sub>30</sub> H <sub>27</sub> Mo <sub>2</sub> NO <sub>4</sub> PRE
mol wt	874.58
cryst syst	triclinic
space group	<i>P</i> $\bar{1}$
radiation ( $\lambda$ , Å)	0.71073
<i>a</i> , Å	11.186(4)
<i>b</i> , Å	15.058(5)
<i>c</i> , Å	9.851(3)
$\alpha$ , deg	79.09(3)
$\beta$ , deg	64.21(2)
$\gamma$ , deg	72.91(3)
<i>V</i> , Å <sup>3</sup>	1424.4(8)
<i>Z</i>	2
calcd density, gcm <sup>-3</sup>	2.039
absorp coeff., mm <sup>-1</sup>	5.198
temperature, K	293(2)
$\theta$ range, deg	3.09 to 30.00
index ranges ( <i>h</i> , <i>k</i> , <i>l</i> )	–13, 15; –20, 21; 0, 13
no. of refls collected	8298
no. of indep refls ( <i>R</i> <sub>int</sub> )	8298 (0.000)
no. of refls with <i>I</i> > 2 $\sigma$ ( <i>I</i> )	6124
<i>R</i> indexes <sup>a</sup> [data with <i>I</i> > 2 $\sigma$ ( <i>I</i> )]	<i>R</i> <sub>1</sub> = 0.0323 <i>wR</i> <sub>2</sub> = 0.0707
<i>R</i> indexes <sup>a</sup> (all data)	<i>R</i> <sub>1</sub> = 0.0554 <i>wR</i> <sub>2</sub> = 0.0768
GOF	0.929
no. of restraints/parameters	0/358

$$^a R_1 = \sum ||F_o| - |F_c|| / \sum |F_o|, wR_2 = [\sum w(F_o^2 - F_c^2)^2 / \sum w(F_o^2)^2]^{1/2}.$$

C<sup>2</sup>(Ph)], 132.2 [d,  $J_{\text{PC}} = 11$ , C<sup>2</sup>(Ph)], 128.9–127.7 (m, Ph), 96.8, 91.1 (2s, Cp), 59.6 [s, C<sup>1</sup>(<sup>t</sup>Bu)], 30.7 [s, C<sup>2</sup>(<sup>t</sup>Bu)]. *Data for compound 6*: Anal. Calcd for C<sub>28</sub>H<sub>29</sub>Mo<sub>2</sub>N<sub>2</sub>O<sub>3</sub>P: C, 51.87; H, 4.51; N, 4.32. Found: C, 51.68; H, 4.72; N, 4.05.  $^1\text{H NMR}$  (200.13 MHz):  $\delta$  7.67–6.76 (m, Ph, 10H), 5.50, 5.31 (2s, 2  $\times$  5H, Cp), 1.45 (s, 9H, Me).  $^{13}\text{C}\{^1\text{H}\}$  NMR (50.33 MHz):  $\delta$  232.5 (d,  $J_{\text{CP}} = 12$ , MoCO), 214.6 (d,  $J_{\text{CP}} = 5$ ,  $\mu\text{-}\eta^1\text{-}\eta^2\text{-CN}$ ), 149.5 [d,  $J_{\text{PC}} = 23$ , C<sup>1</sup>(Ph)], 136.9 [d,  $J_{\text{PC}} = 44$ , C<sup>1</sup>(Ph)], 131.6 [d,  $J_{\text{PC}} = 12$ , C<sup>2</sup>(Ph)], 129.1–128.1 (m, Ph), 99.9, 89.8 (2s, Cp), 62.5 [s, C<sup>1</sup>(<sup>t</sup>Bu)], 32.2 [s, C<sup>2</sup>(<sup>t</sup>Bu)].

**X-ray Structure Determination for Compound 4a.** The intensity data of compound **4a** were collected at room temperature on a Philips PW1100 single-crystal diffractometer using a graphite monochromated Mo K $\alpha$  radiation. Crystallographic and experimental details for the structure are summarized in Table 5. A correction for absorption was made [maximum and minimum values for the transmission coefficients were 1.000 and 0.785].<sup>42</sup> The structure was solved by direct methods and refined by full-matrix least-squares procedures (based on  $F_o^2$ ) with SHELX-97,<sup>43</sup> first with isotropic thermal parameters and then with anisotropic thermal parameters in the last cycles of refinement for all the non-hydrogen atoms. At the end of the isotropic refinement the thermal parameters of the N and O bridging atoms resulted comparable, so confirming the correct position of the bridging atoms. An alternative refinement with the nitride bridging the two molybdenums and the oxo bridging the one Mo and one Re was also carried out, but the thermal parameters of the oxygen and the nitrogen atoms resulted very different (that of the N atom, very high, about three times higher than that of the O atom, very low). The hydrogen atoms were introduced into the geometrically calculated positions and refined riding on the corresponding parent atoms. In the final cycles of refinement a weighting scheme  $w = 1/\sigma^2 F_o^2 + (0.0403P)^2$  where  $P = (F_o^2 + 2F_c^2)/3$ , was used. Full crystallographic data for **4a** are provided in the CIF file format.

(42) (a) Walker, N.; Stuart, D. *Acta Crystallogr.* **1983**, *A39*, 158. (b) Ugozzoli, F. *Comput. Chem.* **1987**, *11*, 109.

(43) Sheldrick, G. M. *SHELX-97. Programs for Crystal Structure Analysis (Release 97-2)*; Institut für Anorganische Chemie der Universität Göttingen: Göttingen, Germany, 1997.

**Computational Details.** All computations described in this work were carried out using the GAUSSIAN03 package,<sup>44</sup> in which the hybrid method B3LYP was applied with the Becke three parameters exchange functional<sup>45</sup> and the Lee–Yang–Parr correlation functional.<sup>46</sup> Effective core potentials (ECP) and their associated double- $\zeta$  LANL2DZ basis set were used for the molybdenum and manganese atoms.<sup>47</sup> The light elements (P, O, C, and H) were described with 6-31G\* basis.<sup>48</sup> Geometry optimizations were performed under no symmetry

(44) Frisch, M. J.; Trucks, G. W.; Schlegel, H. B.; Scuseria, G. E.; Robb, M. A.; Cheeseman, J. R.; Montgomery, Jr., J. A.; Vreven, T.; Kudin, K. N.; Burant, J. C.; Millam, J. M.; Iyengar, S. S.; Tomasi, J.; Barone, V.; Mennucci, B.; Cossi, M.; Scalmani, G.; Rega, N.; Petersson, G. A.; Nakatsuji, H.; Hada, M.; Ehara, M.; Toyota, K.; Fukuda, R.; Hasegawa, J.; Ishida, M.; Nakajima, T.; Honda, Y.; Kitao, O.; Nakai, H.; Klene, M.; Li, X.; Knox, J. E.; Hratchian, H. P.; Cross, J. B.; Bakken, V.; Adamo, C.; Jaramillo, J.; Gomperts, R.; Stratmann, R. E.; Yazyev, O.; Austin, A. J.; Cammi, R.; Pomelli, C.; Ochterski, J. W.; Ayala, P. Y.; Morokuma, K.; Voth, G. A.; Salvador, P.; Dannenberg, J. J.; Zakrzewski, V. G.; Dapprich, S.; Daniels, A. D.; Strain, M. C.; Farkas, O.; Malick, D. K.; Rabuck, A. D.; Raghavachari, K.; Foresman, J. B.; Ortiz, J. V.; Cui, Q.; Baboul, A. G.; Clifford, S.; Cioslowski, J.; Stefanov, B. B.; Liu, G.; Liashenko, A.; Piskorz, P.; Komaromi, I.; Martin, R. L.; Fox, D. J.; Keith, T.; Al-Laham, M. A.; Peng, C. Y.; Nanayakkara, A.; Challacombe, M.; Gill, P. M. W.; Johnson, B.; Chen, W.; Wong, M. W.; Gonzalez, C.; and Pople, J. A. *Gaussian 03*, Revision B.02; Gaussian, Inc.: Wallingford, CT, 2004.

(45) Becke, A. D. *J. Chem. Phys.* **1993**, *98*, 5648.

(46) Lee, C.; Yang, W.; Parr, R. G. *Phys. Rev. B* **1988**, *37*, 785.

(47) Hay, P. J.; Wadt, W. R. *J. Chem. Phys.* **1985**, *82*, 299.

restrictions, using initial coordinates derived from X-ray data of comparable complexes, and frequency analyses were performed to ensure that a minimum structure with no imaginary frequencies was achieved in each case. For interpretation purposes, natural population analysis (NPA) charges<sup>49</sup> were derived from the natural bond order (NBO) analysis of the data.<sup>49</sup> Molecular orbitals and vibrational modes were visualized using the Molekel program.<sup>50</sup> The topological analysis of  $\rho$  was carried out with the Xaim routine.<sup>51</sup>

**Acknowledgment.** We thank the MEC of Spain and Principado de Asturias, Spain, for financial support (Projects CTQ2006-01207 and PA-MAS94-05).

**Supporting Information Available:** Tables of selected molecular orbitals, atomic charges and data from the AIM topological analysis for compound **3b** in pdf format, and full crystallographic data for **4a** in the CIF file format. This material is available free of charge via the Internet at <http://pubs.acs.org>.

(48) (a) Hariharan, P. C.; Pople, J. A. *Theor. Chim. Acta* **1973**, *28*, 213. (b) Petersson, G. A.; Al-Laham, M. A. *J. Chem. Phys.* **1991**, *94*, 6081. (c) Petersson, G. A.; Bennett, A.; Tensfeldt, T. G.; Al-Laham, M. A.; Shirley, W. A.; Mantzaris, J. J. *J. Chem. Phys.* **1988**, *89*, 2193.

(49) Reed, A. E.; Curtis, L. A.; Weinhold, F. *Chem. Rev.* **1988**, *88*, 899.

(50) MOLEKEL: *An Interactive Molecular Graphics Tool*; Portmann, S.; Lüthi, H. P. *CHIMIA* **2000**, *54*, 766.

(51) Ortiz, J. C.; Bo, C. *Xaim*; Departamento de Química Física e Inorgánica, Universidad Rovira i Virgili: Tarragona, Spain, 1998.